electronics

MDPI

Article

Nuclear Island Cable Routing Optimization Based on an Improved A* Algorithm

Wenjing Liu [1], Liang He [1], Yu Ma [1], Xiaopin Yue [1], Yanan Liu [1], Xianghong Liu [1] and Qian Ning [2,*]

[1] State Key Laboratory of Advanced Nuclear Energy Technology, Nuclear Power Institute of China, Chengdu 610213, China
[2] College of Electronics and Information Engineering, Sichuan University, Chengdu 610065, China
* Correspondence: ningq@scu.edu.cn

Abstract

The development of clean and sustainable energy has become a global focus, with nuclear energy playing an important role in low-carbon energy systems. To address the complex cable routing problem in nuclear island environments, this study proposes a three-dimensional cable routing optimization framework based on an improved A* algorithm. The proposed method incorporates multiple engineering-related constraints, including cable type, protection level, turning angle, and construction standards, while optimizing routing paths in constrained spatial environments. A simplified spatial expansion strategy is adopted to approximate routing safety margins while maintaining computational efficiency. Experimental results demonstrate that the proposed method effectively reduces the number of bends and shortens routing paths under predefined engineering constraints, thereby improving routing efficiency and reducing installation costs. The proposed framework provides a preliminary engineering-oriented routing optimization approach and preserves extensibility for future integration of thermal dissipation and electromagnetic compatibility constraints.

Keywords: nuclear island; cable routing; path optimization; A star algorithm

1. Introduction

With increased attention towards sustainable development and climate change mitigation, countries worldwide are actively developing nuclear energy [1]. As primary facilities for nuclear power generation, nuclear power plants require safe and reliable electrical systems, where cables play a crucial role. However, due to the diverse types of equipment and their widespread distribution within nuclear power plants, cable laying becomes difficult and costly [2]. For instance, the first unit of the "Hualong One" Nuclear Power Plant includes approximately 2900 km of cables. Different types of equipment require various specifications and models of cables, making the design and actual construction of cable routes extremely complex. Furthermore, stringent safety protocols mandate physical isolation between different series of cables, thereby exacerbating the complexity of installation and management. Current issues such as overloading of cable trays and unreasonable cable path planning in nuclear power plants substantially inflate construction and maintenance expenditures. Therefore, advanced technological methods must be employed to optimize cable design, improve construction efficiency, and reduce overall costs.

In recent years, significant progress has been made in path-planning algorithms, including Dijkstra's algorithm [3], A* algorithm [4], genetic algorithm [5], particle swarm

Check for updates

Academic Editor: Maciej Ławryńczuk

Received: 17 August 2026
Revised: 8 October 2026
Accepted: 13 October 2026
Published: 23 October 2026

Copyright: © 2026 by the authors. Licensee MDPI, Basel, Switzerland. This article is an open access article distributed under the terms and conditions of the Creative Commons Attribution (CC BY) license.

optimization [6], ant colony algorithm [7], and reinforcement learning algorithm [8]. These algorithms have unique advantages and limitations in different application scenarios.

Many scholars have applied path-planning algorithms to various engineering environments to solve practical problems and have achieved certain results. He et al. [9] proposed two mixed-integer nonlinear programming (MINLP) models for optimizing the topology and routing of pipeline networks in three-dimensional terrain. Wang et al. [10] and Fan et al. [11] used different ant colony algorithms to optimize the routing of ship pipelines. Jinghong Peng et al. [12] used an improved genetic algorithm to optimize the layout of star-shaped gas pipeline networks, considering decision variables such as valve group positions, station arrangements, and pipeline connections to identify the most cost-effective designs. Pires [13] used genetic algorithms (GAs) and integer linear programming (ILP) models to optimize the layout of multiple substations in wind farms and determine the best cable connections to reduce infrastructure costs. Asmara and Nienhuis [14] combined discrete particle swarm optimization (PSO) with Dijkstra's algorithm to establish connection sequences, effectively improving the efficiency of path planning and making full use of the advantages of both algorithms. To minimize the overall cost of wind farm cables, Cazzaro et al. [15] evaluated the performance of simulated annealing, tabu search, variable neighborhood search, ant colony algorithm, and genetic algorithm. Additionally, Wu et al. [16] used an improved ant colony optimization algorithm to design the routing of pipelines between oil and gas processing facilities. Niu et al. [17] used the non-dominated sorting genetic algorithm II (NSGA-II) and co-evolutionary algorithm to solve the optimization problem of ship pipeline layout.

Recent studies have also explored enhancements to A* path planning algorithms, which can be applied to environments such as nuclear islands. Xuan et al. [18] reviewed improvements to A algorithms, focusing on multi-objective optimizations and hybrid methods that improve path quality in complex environments. In a similar vein, Wang et al. [19] incorporated an improved A algorithm with BIM for robotic construction path planning, demonstrating its real-world application. An et al. [20] developed an improved A algorithm on a hexagonal grid to reduce path turns and enhance routing efficiency, which parallels our goal of minimizing bends and path length in cable routing. Li et al. [21] integrated A with a Timed Elastic Band (TEB) strategy for smoother and more efficient motion planning, which is relevant to our method of optimizing the routing for cables in constrained environments. Moreover, Fu [22] examined the use of improved A algorithms for path planning in mobile robotics, highlighting its flexibility in dynamic, real-world settings that share similarities with our nuclear island routing problem. In critical infrastructures, operational integrity and fault diagnosis are also essential. Recent studies on data-driven fault diagnosis in water pipelines based on neuro-fuzzy zonotopic Kalman filters highlight the importance of monitoring and reliability, which motivates the safety-oriented constraints adopted in this work [23].

With the continuous development of path planning algorithms, researchers worldwide have made multifaceted improvements and optimizations to these algorithms for different application scenarios. These improvements have not only enhanced the adaptability of the algorithms under complex conditions but also strengthened their effectiveness in various engineering application environments. Through continuous iteration and optimization of path-planning algorithms, researchers can achieve more precise and economical solutions to specific engineering problems. This ongoing algorithmic innovation enables path-planning algorithms to provide better solutions in complex and changing engineering environments, thereby meeting the demands of practical applications.

Under the premise of meeting the strict safety standards and technical requirements of nuclear power plants, and in response to the issues of large-scale cable laying, complex

laying conditions, and high costs, this study proposes an improved A* algorithm to optimize the cable layout of nuclear power plants, achieve intelligent optimization design of cables, enhance the economy and reliability of nuclear power plants, and make the following contributions:

1. An "extended cable entity" is proposed to model a cable together with its safety isolation zone. This differs from conventional A* improvements that only treat the cable as a single grid or point, because the physical separation among different cable safety categories is explicitly embedded into the routing process.
2. An "energy value" cost term is introduced to encode nuclear-island engineering preferences, including proximity to walls/floors, hazard level, construction difficulty, and maintenance cost. This term is not a modification of the heuristic function; it is embedded into the accumulated cost function $g(n)$.
3. A constrained improved A* algorithm is developed by integrating length, turning, energy, obstacle, and cable-spacing constraints into $g(n)$. The heuristic $h(n)$ remains the unweighted Manhattan distance to preserve admissibility.
4. The method is validated on a real nuclear-island-derived grid model. The experiments are intended as preliminary engineering-oriented verification rather than a large-scale scalability proof.

Table 1 compares representative path-planning and pipeline-routing studies. Unlike prior work that mainly optimizes geometric length or general navigation cost, this study embeds nuclear-island cable safety isolation, turning, and engineering-preference energy terms into the A* cost function.

Table 1. Comparison of representative path-planning and pipeline-routing studies.

Ref.	Method	Application	3D	Main Limitation for Nuclear Cable Routing
[9]	MINLP	Pipeline network	Yes	No cable safety isolation
[10]	GA	Multi-pipe routing	Yes	No nuclear-specific constraints
[18]	Review of A* improvements	General path planning	Yes	No cable-tray or safety spacing model
[20]	Hexagonal A*	Navigation	2D/3D	Turn reduction only, not cable engineering cost
[23]	Neuro-fuzzy zonotopic Kalman filter	Water pipeline fault diagnosis	No	Monitoring/reliability, not routing optimization
This work	Improved A*	Nuclear island cable routing	Yes	Simplified separation approximation; large-scale scalability left as future work

The structure of this paper is as follows. The first section serves as the introduction, presenting the background, objectives, scope, and significance of the research, as well as an overview of related work both domestically and internationally, and the structure of the paper. The second section introduces the mathematical model developed for intelligent cable-routing design in nuclear power plants. The third section focuses on the experimental methods used in this study, detailing the principles and implementation strategies. The fourth section presents the results of applying the proposed method to a part of the nuclear island structure, while the fifth section summarizes the research and discusses existing challenges.

2. Problem Modeling

2.1. Cabling Space and Cables

Within a nuclear island's cabling space, there exists a variety of equipment and devices. To facilitate modeling and analysis, these components were approximated as rectangular shapes. The entire cabling space of the nuclear island was discretized using a grid-based approach. Based on the minimum diameter of the cables, the cabling space was divided into cubic grids, with the edge length of each grid set to one in the model. Two attributes are assigned to each grid: if a grid is occupied by equipment or designated as a cabling prohibition zone, it is marked as an obstacle grid; otherwise, it is considered as a free grid. For free grids, an energy value is assigned, where a lower energy value indicates a higher preference for cable routing within that grid, such as grids near walls or floors, which can reduce the cost of cable support and construction during installation. The details are provided in Section 2.2.3. After grid division of the cabling space is completed, the grid at the lower left corner of the cabling space is designated as the origin (0, 0, 0). The coordinates of the kth grid through which a cable path passes are denoted as (x_k, y_k, z_k).

This study presents the actual cable routing paths using a single grid that approximates their diameter and denotes the cable paths using grid coordinates, as shown in Equation (1).

$$C_1 : g_1(x_1, y_1, z_1), g_2(x_2, y_2, z_2), ..., g_n(x_n, y_n, z_n) \quad (1)$$

C_1 represents the first cable, where g_1 denotes the starting grid coordinates of the cable path for C_1 and g_n represents the ending grid coordinates.

In nuclear power plants, cables are categorized based on their voltage levels and function as medium-voltage (MV), low-voltage (LV), control (C), measurement (M), and utility (P) cables. The additional details are provided in Table 2. Each type of cable has specific installation requirements, such as the use of different cable trays and the need to maintain a certain spacing between the cables. To ensure overall safety, power plants are designed with high reliability and redundancy. Cables are divided into multiple safety categories based on their different safety levels and electrical isolation requirements. Separate cable trays must be designed for different safety categories to meet the isolation requirements. In the proposed optimization framework, cables with higher safety priorities are routed first, while already installed cables are treated as obstacles for subsequent routing. This ensures that the installed paths are not disturbed, and the routing of new cables adheres to safety and operational constraints. The algorithm accommodates these priorities by treating different cable systems as separate functional entities and adjusting the routing strategy accordingly.

Table 2. Cable types, safety categories, and typical quantitative information.

Cable Type	Safety Category	Num	Outer Diameter (mm)	Minimum Spacing (mm)
Medium voltage cable (MV)	A	1	30–60	≥200
	B	1	30–60	≥200
Low voltage cable (LV)	A	1	15–40	≥200
	B	1	15–40	≥200
Control cable (C)	A	1	8–20	≥150
	B	1	8–20	≥150
	C	1	8–20	≥150
Measure cable (M)	A	1	6–15	≥150
	B	1	6–15	≥150
	C	1	6–15	≥150
Public utility cable (P)	A	1	10–25	≥200
	B	1	10–25	≥200

Minimum spacing refers to the required separation between cable trays of different safety categories. The values are typical engineering references and should be adapted to specific plant specifications.

2.2. Objective Function

2.2.1. Length

In practical cable installation, the length of the cable route is a significant factor affecting the overall construction cost of a nuclear island. Analysis of cable installation costs in nuclear power plants indicates that the total cost includes the cost of the cables themselves, cable trays, labor costs, and cable-laying expenses. While the cost of the cables accounts for only 20% of the total expenses, the remaining costs are closely related to the actual length of the cables. Therefore, minimizing cable length is a key objective. In this model, the cable installation path is directly simplified to a grid space that represents the cable, where the number of grids corresponds to the cable length. The objective function is given by Equation (2).

$$minF_L = \sum_{i=1}^{N} C_i(n) \tag{2}$$

where F_L is the total length of the cable path, N is the number of cables, and

$$C_i(n) = \sum_{j=1}^{n_i} 1 \tag{3}$$

is the number of grids traversed by cable i, i.e., the discrete cable length.

2.2.2. The Number of Bends

In cable installation within a nuclear island, cables rely on trays for support. However, cable trays have fixed design specifications, and owing to their material properties, strict requirements are imposed on the bending of cable routes in practical applications. If the installation path involves bends, it significantly increases the cost of cable trays and labor expenses for installation. Therefore, minimizing cable bends is crucial for designing cable installation routes. The model proposed in this study records the number of turns in the generated path, with fewer turns indicating a better-designed route.

$$minF_B = \sum_{i=1}^{N} C_i(b) \tag{4}$$

where F_B is the total number of turns in the cable path, and

$$C_i(b) = \sum_{j=2}^{n_i} I(\mathrm{dir}_j \neq \mathrm{dir}_{j-1}) \tag{5}$$

is the number of direction changes in cable i, with $I(\cdot)$ being the indicator function.

2.2.3. Energy Value

The overall design of a nuclear island is highly complex and features numerous intricate facilities and pipelines. This paper introduces the concept of energy values in the grid attributes of the cable installation space to assist in identifying and avoiding interference from other equipment and mitigating safety issues arising from an improper cable layout. Regions deemed more 'hazardous' or less suitable for cable installation were assigned higher energy values. Conversely, the areas near the walls within the cable installation space were designated as low-energy value zones. This approach aims to reduce the material usage and installation costs associated with cable trays as well as to minimize the complexity of the future maintenance and repair of cables. Energy values are assigned according to the Equation (6), where e is the energy value, d is the distance to the nearest obstacle and k is a constant used to adjust the scaling factor. The energy value

increases as the distance increases, ensuring that the cable path stays closer to walls. As shown in Equation (7), the total energy value of the cable path is used as an optimization objective, with the goal of achieving the lowest possible total energy value.

$$e = kd \tag{6}$$

$$minF_E = \sum_{i=1}^{N} \sum_{j=1}^{n_i} C_i(e_j) \tag{7}$$

where F_E is the total energy value of the cable path, N is the number of cables, n_i is the length of the ith cable, and $C_i(e_j)$ is the energy value of the jth grid in the path of the ith cable.

Equation (9) summarizes the objective function of the final model. This function considers the length of the cable path, number of turns, and energy value to minimize the overall costs and optimize the path design.

$$F_L = \sum_{i=1}^{N} C_i(n), \quad F_B = \sum_{i=1}^{N} C_i(b), \quad F_E = \sum_{i=1}^{N} \sum_{j=1}^{n_i} C_i(e_j) \tag{8}$$

$$F_{\text{obj}} = \alpha F_L + \beta F_B + \gamma F_E \tag{9}$$

where F_{obj} is the total objective function that we aim to minimize, and α, β, γ are the weight coefficients. The weight coefficients (α, β, γ) in the objective function were determined through a combination of experimental sensitivity analysis and expert input, ensuring that the trade-offs between length, bends, and energy were appropriately balanced based on the specific needs of nuclear island cable routing.

2.3. Constraints

2.3.1. Orthogonal Cabling

In the three-dimensional space of a nuclear island, cable path design is typically constrained by the layout of the cabling space, such as equipment, walls, floors, and ceilings. Orthogonal path searching restricts the search direction to only six basic directions (up, down, left, right, forward, and backward), as shown in Equation (7). This approach simplifies the problem and reduces the computational complexity. In practical engineering projects, cable path design often needs to follow the layout of the building structure. Orthogonal path searching is more in line with actual cabling requirements because it can effectively avoid obstacles, minimize cable bends and crossings, and reduce costs and complexity.

$$\begin{aligned} (x_i, y_i, z_i) = {} & (x_{i-1} \pm 1,\ y_{i-1},\ z_{i-1}) \\ & \text{or } (x_{i-1},\ y_{i-1} \pm 1,\ z_{i-1}) \\ & \text{or } (x_{i-1},\ y_{i-1},\ z_{i-1} \pm 1) \end{aligned} \tag{10}$$

where (x_i, y_i, z_i) is the coordinate of the currently selected cable path grid and $(x_{i-1}, y_{i-1}, z_{i-1})$ are the coordinates of the previously determined grid in the cable path. This implies that the cable path must select a grid coordinate in the direction orthogonal to the previous path grid as the current available path.

Orthogonal routing is adopted because nuclear-island cables are normally supported by trays along walls, floors, and ceilings. If non-orthogonal laying is permitted in some engineering scenarios, the search neighborhood can be extended to 45° or arbitrary directions, and an angle-dependent penalty can be added to $g(n)$. Alternatively, a post-processing smoothing step can be used. However, such relaxation must still satisfy the minimum bending radius and tray-support requirements.

2.3.2. Obstacle Constraints

In the design of cable paths, it is crucial to ensure that cable routing does not interfere with existing equipment or obstacles within the space. To effectively manage this problem, specific values were assigned to the grid attributes corresponding to these obstacles. When searching for the optimal cable path, the algorithm first checks whether a given grid cell is an obstacle. If it is, the cell is excluded from considering the cable path, as shown in Equation (8). This approach ensures a clear distinction between available and unavailable areas, thereby enhancing the reliability and safety of the cable installation process.

$$O(x_i, y_i, z_i) \neq 1 \tag{11}$$

$O(x_i, y_i, z_i)$ indicates whether the grid at coordinates (x_i, y_i, z_i) is an obstacle.

2.3.3. Cable Spacing Constraints

In nuclear power plants, cables are categorized into five types based on their voltage and specific functions, as detailed in Table 2. Owing to the inherent requirements of high reliability and redundancy in the operation of nuclear power plants, specific spacing requirements must be observed during the design process. Specifically, different types of cables must not be installed in the same cable tray, and sufficient spacing must be maintained between cable trays carrying different types of cables. Additionally, to ensure that the reactor protection system effectively fulfills its nuclear safety functions, an extra safety series is incorporated into the design. This ensured that the reactor protection system responded appropriately under all conditions. Therefore, cable trays for different safety series must be independently designed to meet the isolation requirements, thereby enhancing the overall safety and integrity of the nuclear facility.

In the proposed model, we implement an expansion mechanism for the designed cables, as shown in Figure 1. Through this mechanism, the original grid occupied by a cable is enlarged to include the target grid and its eight surrounding grids, thereby introducing a simplified spatial clearance around each routed cable. This grid expansion is used as a simplified approximation of cable separation requirements for path planning, ensuring that candidate routing paths satisfy a minimum grid-based spacing criterion, as described in Equation (9). This approach results in a cross-sectional representation of the cable path occupying a total of nine grid cells. By doing so, this method provides a simplified approximation of cable spatial requirements and routing safety margins while preserving computational tractability in large-scale constrained environments. This strategy facilitates the analysis of potential routing interferences and provides an extensible basis for incorporating additional engineering constraints, such as thermal dissipation and electromagnetic compatibility requirements, in future developments.

$$\min_{j \in N_n} \sqrt{(x_i - x_j)^2 + (y_i - y_j)^2 + (z_i - z_j)^2} > d \tag{12}$$

where N_n denotes the set of grid cells occupied by previously routed cable paths, and d denotes the minimum grid-based separation distance required between cable paths. It should be noted that this spacing criterion is intended to provide a computationally efficient approximation of cable isolation requirements for routing optimization rather than a complete physical model considering thermal dissipation or electromagnetic compatibility.

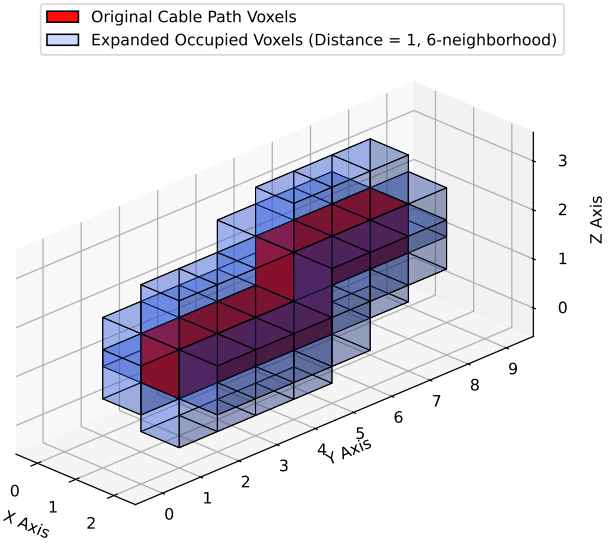


Figure 1. Illustration of the grid expansion for cable routing. Red voxels represent the grid cells actually occupied by the original cable path. Blue translucent voxels represent the surrounding grid cells expanded to an occupied state because their distance to the original cable is exactly 1 (6-neighborhood connectivity). Free grid cells are omitted for clarity.

3. Solution

The A* algorithm was developed by Hart et al. [4] in 1968, has undergone several enhancements, and has become widely used in various pathfinding scenarios. Among the existing path search algorithms, A* is considered to be one of the most efficient direct search algorithms, characterized by completeness and optimality. The A* algorithm is based on Dijkstra's algorithm and the best-first search algorithm, and maintains a framework that relies on systematic search exploration. By using a cost estimation function, A* can make efficient pathfinding decisions, gradually expanding the child nodes around the parent node, and progressively approaching the goal node. The evaluation function is a core component of the A* algorithm and consists of two main parts: $g(n)$, which represents the actual cost from the starting node to the current node, and $h(n)$, which represents the heuristic cost from the current node to the goal node. The evaluation function is typically defined by the following Equation (13).

$$f(n) = g(n) + h(n) \tag{13}$$

To improve the efficiency and effectiveness of the cable path design process under the unique constraints of the nuclear island environment, we combined the practical application scenarios of cables in the nuclear island and optimized the evaluation function $g(n)$ based on the content in Section 2. Function $f(n)$ is similar to the objective function. Meanwhile, $h(n)$ is defined as the Manhattan distance from the current grid to the destination grid. The heuristic function is intentionally left unweighted to preserve the admissibility and computational efficiency of the A* search, while the routing preferences are incorporated through the accumulated cost function $g(n)$.

$$g(n) = \alpha L(n) + \beta B(n) + \gamma E(n), \qquad \alpha = 1,\ \beta = 5,\ \gamma = 1 \tag{14}$$

$$h(n) = |x_n - x_d| + |y_n - y_d| + |z_n - z_d| \tag{15}$$

where $L(n)$ denotes the accumulated routing length, $B(n)$ denotes the accumulated turning penalty, and $E(n)$ represents the accumulated energy cost of the traversed grids. According to the implementation of the proposed algorithm, the weighting coefficients are fixed as

$\alpha = 1$, $\beta = 5$, and $\gamma = 1$ throughout all experiments. The weights are selected based on engineering practice and sensitivity analysis. A unit length and a unit energy value are both normalized to one grid step, so $\alpha = \gamma = 1$. A turn is penalized as five grid steps ($\beta = 5$), reflecting the additional tray and labor cost caused by bending. (x_n, y_n, z_n) and (x_d, y_d, z_d) represent the coordinates of the current grid and the destination grid, respectively.

The evaluation function combines the accumulated routing cost and the heuristic estimate to guide the search toward feasible routing solutions under the predefined engineering constraints.

If the open set becomes empty before the goal is reached, the algorithm returns no feasible path. In practice, the last expanded node and blocked region can be logged to help engineers identify congestion or over-constrained isolation zones. In highly congested narrow spaces, the expanded cable entity may occupy all available free grids, and the algorithm will correctly report infeasibility rather than returning an invalid path.

The flowchart of the algorithm is shown in Figure 2.

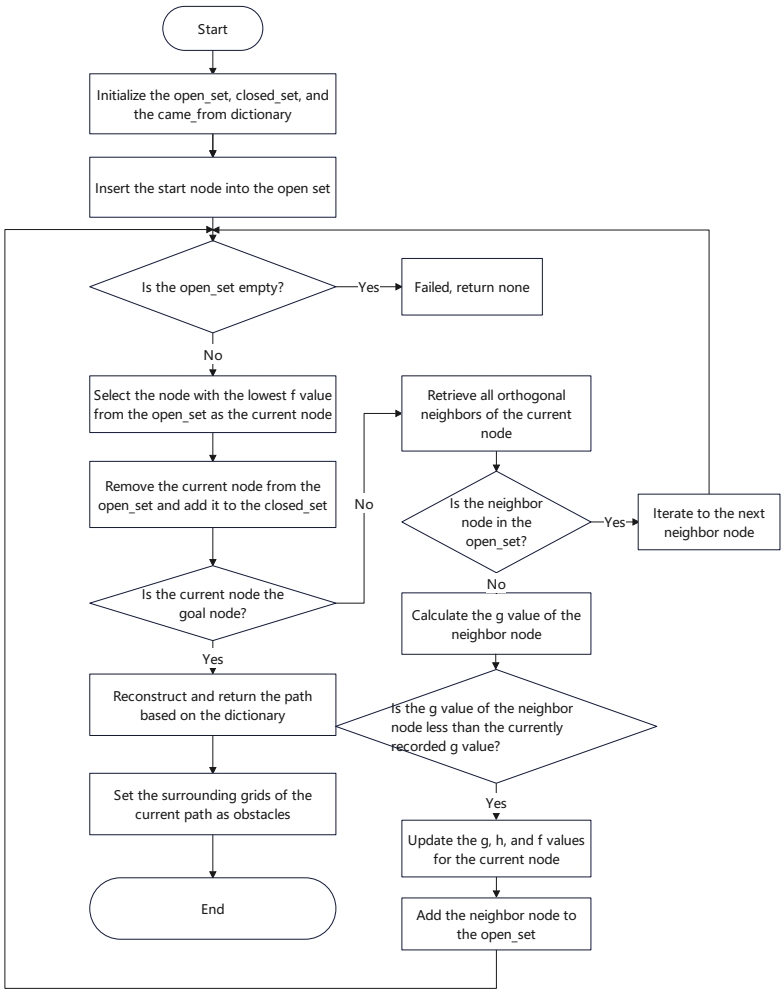


Figure 2. Flow chart of improved A* algorithm. In each iteration, the algorithm (i) retrieves orthogonal neighbors, (ii) checks obstacle constraints, (iii) rejects neighbors inside expanded cable entities, (iv) accumulates length, turning, and energy costs, and (v) updates the open set. If the open set becomes empty, infeasibility is reported.

4. Simulation Experiment

4.1. Experimental Environment

The equipment and software platform used in the experimental phase of this study were Intel i7-10700 CPU and Python 3.12. In the simulation experiments in this study, a

grid-based method was employed to construct the environmental model for cable routing, with the following specifications: In the created three-dimensional grid map, red represents obstacles with known size and position, and white represents the free grid, where cables can be selected as paths. All free grids were assigned an energy value based on their distance from obstacles, and the energy value decreased as the distance to the obstacle decreased.

In the experiment described in this section, we created a three-dimensional grid space of size $100 \times 100 \times 100$. The starting coordinates of the three cables were set as (0, 99, 99), (0, 0, 60), and (0, 0, 0), and the corresponding destination coordinates were (99, 60, 0), (60, 0, 40), and (99, 50, 0). Because the entire grid map is positioned in the Cartesian coordinate system, each grid node can be uniquely identified by its corresponding path point coordinates (x, y, z).

The parameter settings are summarized in Table 3.

Table 3. Parameter settings used in the experiments.

Algorithm/Parameter	Value	Description
Improved A (from implementation)*		
Search directions	6 orthogonal	$(\pm x, \pm y, \pm z)$
Heuristic	Manhattan distance	Unweighted
Step cost	1	$\alpha = 1$
Turning penalty	5	$\beta = 5$
Energy weight	1	$\gamma = 1$
Energy value	$e = kd, k = 1$	Precomputed
Open set	Binary heap	`Heap queue`
RRT (comparison)		
Iterations	100,000	Section 4.2
Step size	1	Section 4.2
PSO (comparison)		
Iterations	50	Section 4.2
Swarm size	30	Section 4.2
Inertia weight	0.5	Section 4.2
Environment		
Simulation grid	$100 \times 100 \times 100$	Section 4.1
Case-study grid	$97 \times 119 \times 23$	Section 4.3
CPU	Intel i7-10700	Section 4.1
Programming language	Python 3.12	Section 4.1

4.2. Comparison Experiment of Different Algorithms

In this subsection, we perform cable routing using the original A* algorithm, Rapidly-exploring Random Tree (RRT) algorithm, Particle Swarm Optimization (PSO) algorithm, and the proposed improved A* algorithm in the three-dimensional space described in Section 4.1. The RRT algorithm runs for 100,000 iterations with a step size of 1, the PSO algorithm runs for 50 iterations with a swarm size of 30 and an inertia weight of 0.5 is used. The routing results are shown in Figure 3, and a comparison of the cable path data is presented in Table 4 and Figure 4 .

The results in Table 4 and Figure 3 indicate that all four algorithms can effectively accomplish the routing task. Compared with the original A*, the improved A* reduces runtime from 267.19 s to 14.49 s and reduces energy from 4813 to 1989. Its bend count is close to the original A* and much lower than RRT and PSO. The RRT algorithm exhibited the quickest response time and generated the shortest paths; however, its inherent randomness led to the highest number of bends and insufficient practical path optimization. The original A* algorithm performs better in terms of path length, but underperforms in terms of the

number of bends and time taken. Although the PSO algorithm performs well in terms of bends and energy values, it requires multiple iterations, leading to a significant increase in runtime. After 15 iterations, it becomes stuck in a local optimum, and the increased time cost does not improve the path-planning results.

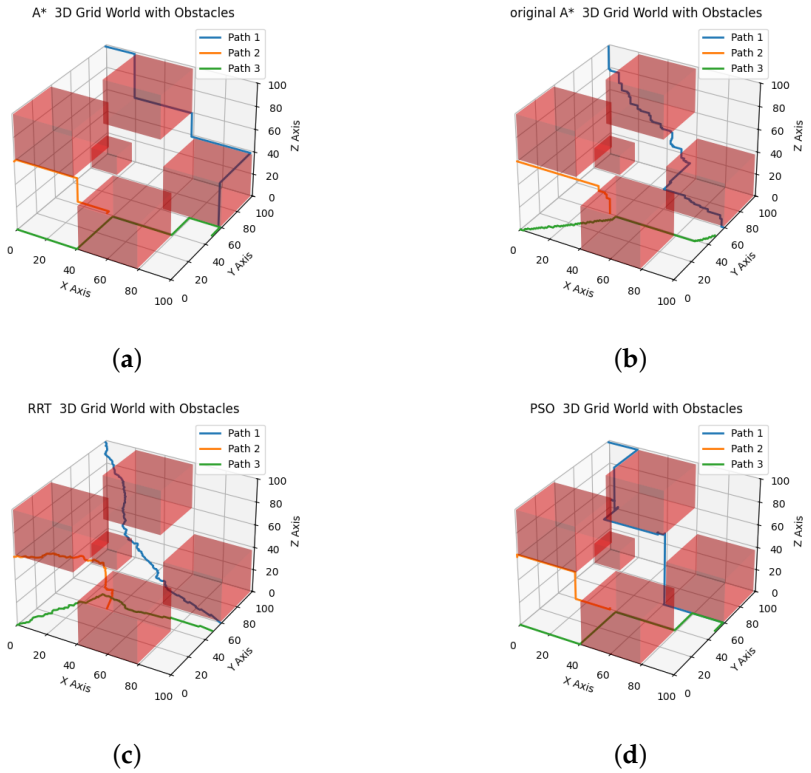


Figure 3. Comparison of different algorithms. (**a**) Improved A*. (**b**) Original A*. (**c**) RRT. (**d**) PSO.

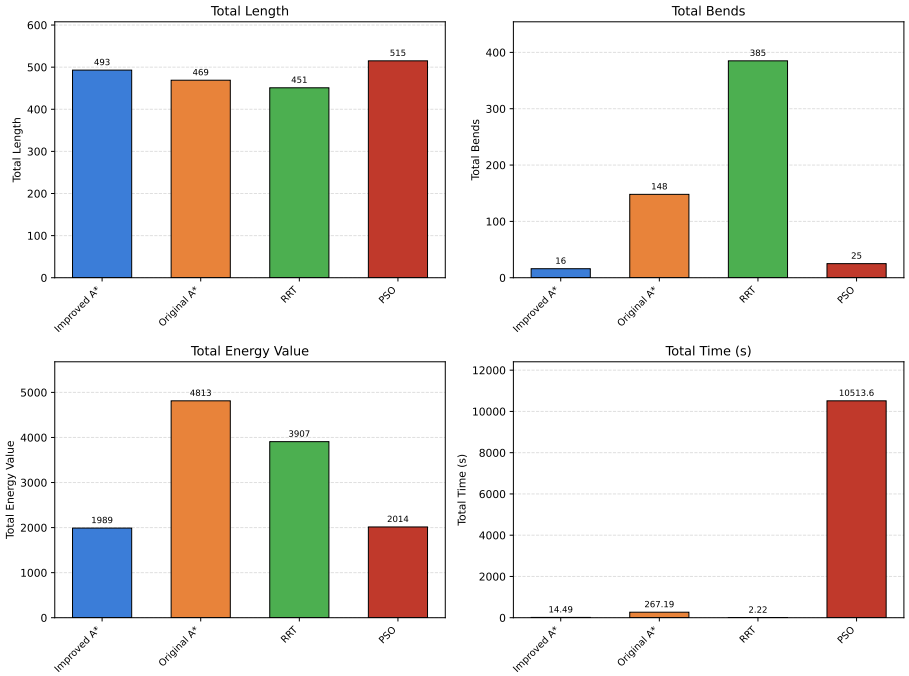


Figure 4. Algorithm comparison.

Table 4. Performance comparison of different algorithms.

Algorithm	Total Length	Total Bends	Total Energy	Time (s)	Relative Time
Improved A*	493	16	1989	14.49	1.00
Original A*	469	148	4813	267.19	18.44
RRT	451	385	3907	2.22	0.15
PSO	515	25	2014	10,513.61	725.58

Compared to other algorithms, the improved A* algorithm can significantly reduce the number of bends in a short period and attempt to follow walls for routing. Its total path length is comparable to that of other traditional algorithms, demonstrating its higher practicality.

4.3. Case Application

To further validate the effectiveness of the mathematical model and solving algorithm, a portion of the nuclear island structure was extracted and divided into a $97 \times 119 \times 23$ grid space, with grid coordinates representing its spatial layout.

This study considers three routing scenarios. Scenario 1: Routing of three cables with the same starting point and different endpoints (all three cables belong to the same safety series). Scenario 2: Routing of three cables with the same endpoint and different starting points (all three cables belong to the same safety series), where the starting and ending points, in this case, are exactly opposite to those in Scenario 1. Scenario 3: Routing of 12 cables listed in Table 2.

4.3.1. Impact of Energy Value on Cable Routing Results

In the improved A* algorithm, the cost function incorporates the concept of energy values in the routing space, aiming to make the cable path closer to the walls for easier cable bracket installation and to reduce the construction costs. The distribution of the energy values in the grid space available for routing on a nuclear island is shown in Figure 4. To verify the impact of this setting, two experiments were conducted for Scenario 1: one with the energy value calculation retained in the cost function, and one with the energy value removed, both within the same experimental environment. The results are shown in Figure 5.

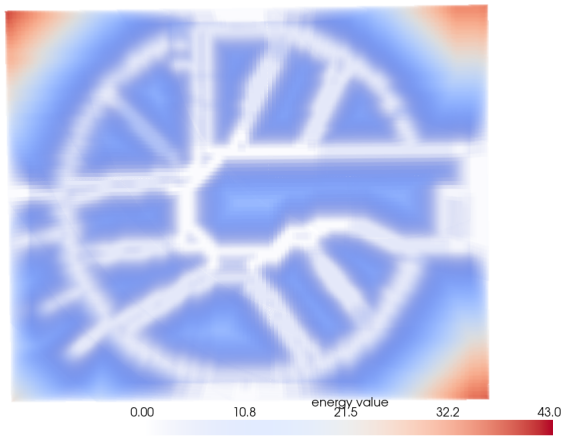


Figure 5. Energy Value Distribution of Routing Space.

By comparing the routing effects in Figure 6, it is clear that when the energy value objective is omitted. However, the number of path bends was reduced, and the path's proximity to the wall decreased. In practical applications, such as nuclear power plants,

this will significantly increase the difficulty and cost of cable bracket installation. This comparison further proves the necessity and effectiveness of incorporating an energy value set into the cost function.

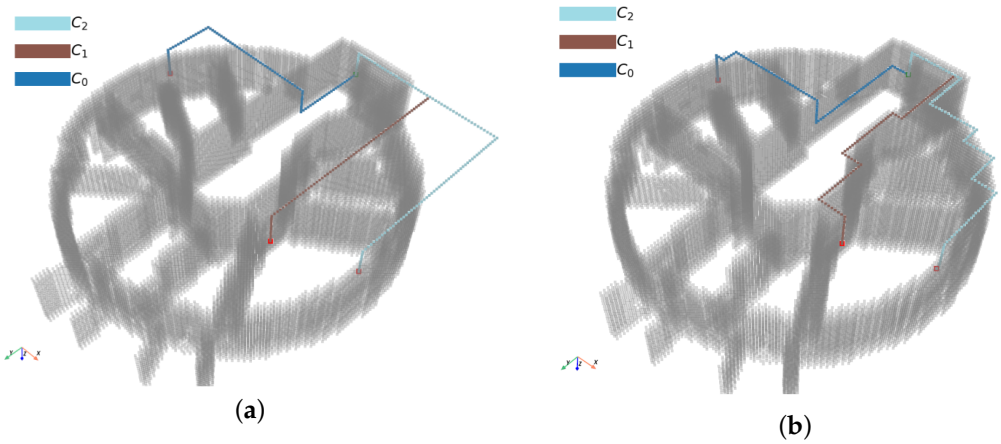


Figure 6. Comparison of results: (**a**) without energy value; (**b**) with energy value.

4.3.2. Cable Routing Results Under Different Scenarios

For the three routing scenarios presented in Section 4.2, the improved A* algorithm was used to optimize the cable routes for the nuclear island. The cable paths for Scenarios 1 and 2 are shown in Figure 7, and the path data are presented in Table 5. When the starting and ending points were completely reversed, the paths remained almost unchanged, validating the effectiveness and reliability of the routing method. In Scenario 3, we considered a more complex situation with 12 cables of different functions and a safety series starting from different points and reaching different endpoints. A visualization of the experimental results is shown in Figure 8. The path data are listed in Table 5, demonstrating the versatility and adaptability of the routing method.

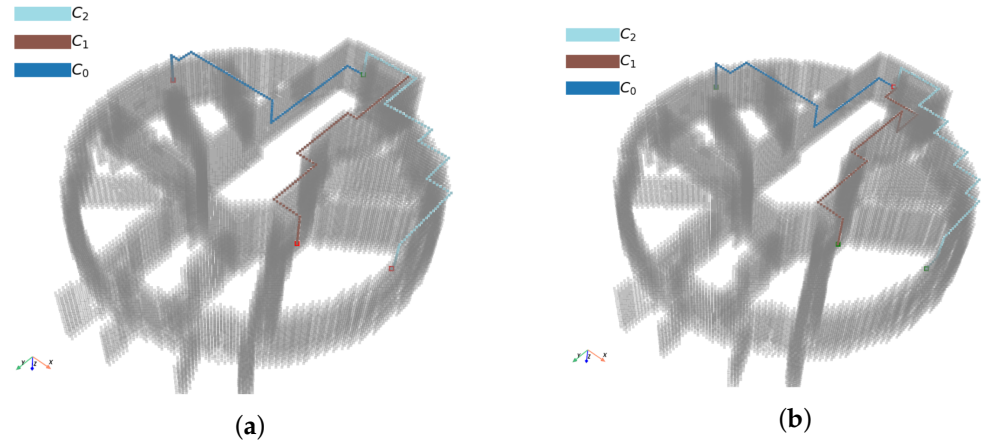


Figure 7. Routing Results: (**a**) Scenario 1; (**b**) Scenario 2.

The cable routing method proposed in this study performed excellently in tasks with different starting and ending points. From the visualized results, it can be seen that the grid energy value setting effectively ensures that the cable paths are routed close to the walls, thereby reducing the construction cost of the subsequent cable brackets. In the complex case of Scenario 3, the total runtime of the program is 11.07 s, with an average routing time of approximately 0.92 s per cable. The 12 cables have an average length of 91.17 grids, an average of 7.17 bends, and an average energy value of 139.67. These descriptive statistics are derived from the existing experimental data. This is significantly

faster than traditional manual routing, which greatly improves routing efficiency. The routing results can be visualized in an intelligent routing system, allowing engineers to easily observe and make adjustments.

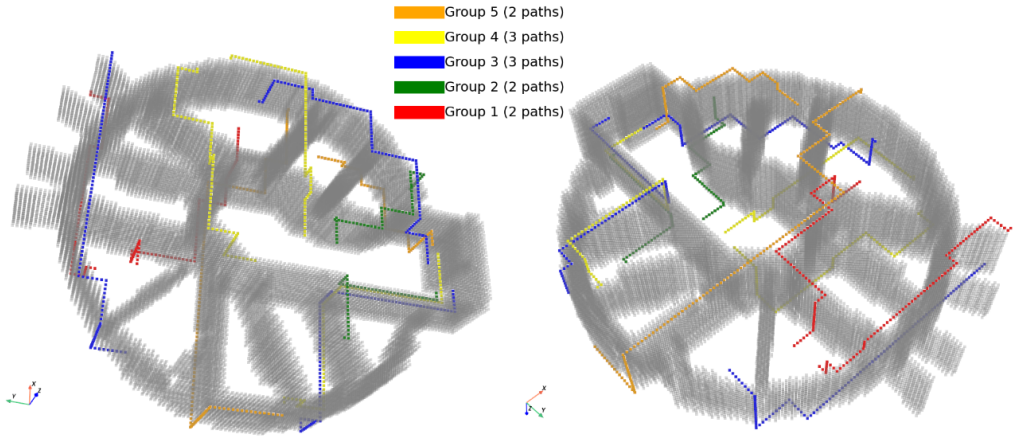


Figure 8. Routing Results for Scenario 3.

Table 5. Path data for different scenarios.

Scenario	Cable	Length	Bends	Energy Value
Scenario 1	C_0	98	6	114
	C_1	113	8	122
	C_2	119	10	137
	Total	330	24	373
Scenario 2	C_0	98	6	118
	C_1	107	9	132
	C_2	119	13	131
	Total	324	28	381
Scenario 3	C_0	77	9	110
	C_1	91	8	173
	C_2	52	4	59
	C_3	62	7	111
	C_4	103	4	175
	C_5	98	6	114
	C_6	109	10	149
	C_7	95	9	139
	C_8	101	7	137
	C_9	81	6	178
	C_{10}	72	9	126
	C_{11}	153	7	205
	Mean	91.17	7.17	139.67
	Std.	26.10	1.95	39.60

5. Conclusions

This study demonstrates that the improved A* algorithm can effectively optimize cable routing paths in constrained three-dimensional nuclear island environments. By comprehensively considering factors such as cable installation length, bending radius, distance from walls, and spacing requirements between different cables, the proposed method improves routing efficiency while reducing construction costs. Experimental results show that the algorithm can generate feasible routing solutions more efficiently than traditional manual wiring approaches under predefined engineering constraints. Compared with conventional methods relying heavily on engineering experience, the

improved A* algorithm provides a more efficient routing optimization framework for complex cable layout scenarios.

To maintain computational efficiency and model tractability in large-scale environments, this study adopts a simplified spatial expansion strategy to approximate cable safety margins and routing separation requirements. Although thermal load and electromagnetic interference are not explicitly modeled in the current work, the proposed framework preserves extensibility for incorporating thermal dissipation and electromagnetic compatibility penalty constraints. The objective can be extended as

$$F_{\text{obj}} = \alpha F_L + \beta F_B + \gamma F_E + \delta F_T + \varepsilon F_{\text{EMC}}. \tag{16}$$

For thermal constraints, a penalty can be defined as

$$F_T = \sum_j \lambda_T \max(0, T_j - T_{\max})^2, \tag{17}$$

where T_j is the local temperature and $T_{\max}$ is the allowable limit. For EMC, a distance-based penalty can be used:

$$F_{\text{EMC}} = \sum_j \frac{\lambda_{\text{EM}}}{d_{\text{EM},j}^2}, \tag{18}$$

or an interference-threshold penalty $F_{\text{EMC}} = \sum_j \lambda_{\text{EM}} \max(0, I_j - I_{\text{th}})^2$. These terms can be directly added to $g(n)$ in future implementations.

Future research may further investigate the integration of multi-physics routing constraints, including thermal loading, electromagnetic compatibility, and emergency risk factors such as fire and flooding. In addition, larger-scale nuclear island models and more complex routing scenarios will be considered to further evaluate the scalability and applicability of the proposed framework in practical engineering environments. The improved A* has the same asymptotic complexity as standard A*. For much larger grids and hundreds of cables, hierarchical search, jump-point search, parallelization, and candidate-path caching can be considered.

Author Contributions: Conceptualization, W.L.; Methodology, W.L.; Software, W.L.; Validation, W.L.; Formal analysis, W.L.; Investigation, L.H.; Resources, L.H.; Data curation, L.H.; Writing—original draft, L.H.; Writing—review & editing, Y.M.; Visualization, Y.M., X.Y. and X.L.; Supervision, X.Y., Y.L., X.L. and Q.N.; Project administration, X.Y. and Q.N. All authors have read and agreed to the published version of the manuscript.

Funding: This research received no external funding.

Data Availability Statement: Due to privacy concerns, the data cannot be obtained.

Conflicts of Interest: The authors declare no conflicts of interest.

References

1. Davenport, J.; Wayth, N. *Statistical Review of World Energy*; Energy Institute: London, UK, 2023.
2. Hashemian, H.M. Nuclear power plant instrumentation and control. In *Nuclear Power–Control, Reliability and Human Factors*; InTech: London, UK, 2011; pp. 49–66.
3. Dijkstra, E.W. A note on two problems in connexion with graphs. In *Edsger Wybe Dijkstra: His Life, Work, and Legacy*; Springer: Berlin/Heidelberg, Germany, 2022; pp. 287–290.
4. Hart, P.E.; Nilsson, N.J.; Raphael, B. A formal basis for the heuristic determination of minimum cost paths. *IEEE Trans. Syst. Sci. Cybern.* **1968**, 4, 100–107. [CrossRef]
5. Holland, J.H. Genetic algorithms. *Sci. Am.* **1992**, *267*, 66–73. [CrossRef]
6. Kennedy, J.; Eberhart, R. Particle swarm optimization. In *Proceedings of the ICNN'95*; IEEE: Piscataway, NJ, USA, 1995; Volume 4, pp. 1942–1948.

7. Dorigo, M. Optimization, Learning and Natural Algorithms. Ph.D. Thesis, Politecnico di Milano, Milan, Italy, 1992.
8. Toorchi, N.; Lyu, W.; He, L.; Zhao, J.; Rasheed, I.; Hu, F. Deep reinforcement learning enhanced skeleton based pipe routing for high-throughput transmission in flying ad-hoc networks. *Comput. Netw.* **2024**, *244*, 110330. [CrossRef]
9. He, G.; Li, Y.; Lin, M.; Liao, K.; Liang, Y. Optimization of gathering and transmission pipe network layout in gas field and pipeline route in 3D terrain. *J. Pipeline Syst. Eng. Pract.* **2019**, *10*, 04019009. [CrossRef]
10. Wang, H.; Zhao, C.; Yan, W.; Feng, X. Three-dimensional multi-pipe route optimization based on genetic algorithms. In *Knowledge Enterprise: Intelligent Strategies in Product Design, Manufacturing, and Management*; Springer: Berlin/Heidelberg, Germany, 2006; pp. 177–183.
11. Wang, Y.-L.; Yu, Y.-Y.; Li, K.; Zhao, X.-G.; Guan, G. A human-computer cooperation improved ant colony optimization for ship pipe route design. *Ocean Eng.* **2018**, *150*, 12–20. [CrossRef]
12. Peng, J.; Zhou, J.; Liang, G.; Qin, C.; Peng, C.; Chen, Y.; Hu, C. Global layout optimization of star-tree gas gathering pipeline network via an improved genetic optimization algorithm. *J. Intell. Fuzzy Syst.* **2023**, *44*, 2655–2672. [CrossRef]
13. Pires, E.J.S.; Cerveira, A.; Baptista, J. Wind farm cable connection layout optimization using a genetic algorithm and integer linear programming. *Computation* **2023**, *11*, 241. [CrossRef]
14. Asmara, A.; Nienhuis, U. Automatic piping system in ship. In Proceedings of the International Conference on Computer and IT Application (COMPIT), Oegstgeest, The Netherlands, 8–11 May 2006; pp. 269–280.
15. Cazzaro, D.; Fischetti, M.; Fischetti, M. Heuristic algorithms for the wind farm cable routing problem. *Appl. Energy* **2020**, *278*, 115617. [CrossRef]
16. Wu, L.; Tian, X.; Wang, H.; Liu, Q.; Xiao, W. Improved ant colony optimization algorithm and its application to solve pipe routing design. *Assem. Autom.* **2019**, *39*, 45–57. [CrossRef]
17. Niu, W.; Sui, H.; Niu, Y.; Cai, K.; Gao, W. Ship pipe routing design using NSGA-II and coevolutionary algorithm. *Math. Probl. Eng.* **2016**, *2016*, 7912863. [CrossRef]
18. Xuan, D.T.; Hung, N.T.; Thang, V.T. A Comprehensive Review of Improved A* Path Planning Algorithms and Their Hybrid Integrations. *Automation* **2025**, *6*, 52. [CrossRef]
19. Wang, D.; Liu, B.; Jiang, H.; Liu, P. Path Planning for Construction Robot Based on the Improved A* Algorithm and Building Information Modeling. *Buildings* **2025**, *15*, 719. [CrossRef]
20. An, Z.; Rui, X.; Gao, C. Improved A* Navigation Path-Planning Algorithm Based on Hexagonal Grid. *ISPRS Int. J. Geo-Inf.* **2024**, *13*, 166. [CrossRef]
21. Li, X.; Li, T.; Zhang, Y.; Li, Z.; Ban, L.; Sun, K. A-TEB: An Improved A Algorithm Based on the Timed Elastic Band Strategy for Motion Planning. *Sensors* **2025**, *25*, 6117. [PubMed]
22. Fu, X. Research on Path Planning of Mobile Robots Based on Improved A* Algorithm. *PeerJ Comput. Sci.* **2025**, *11*, e2691. [CrossRef] [PubMed]
23. Pérez-Pérez, E.J.; González-Baldizón, Y.; Fragoso-Mandujano, J.A.; Guzmán-Rabasa, J.A.; Santos-Ruiz, I. Data-driven fault diagnosis in water pipelines based on neuro-fuzzy zonotopic Kalman filters. *Math. Comput. Appl.* **2025**, *30*, 2. [CrossRef]

Disclaimer/Publisher's Note: The statements, opinions and data contained in all publications are solely those of the individual author(s) and contributor(s) and not of MDPI and/or the editor(s). MDPI and/or the editor(s) disclaim responsibility for any injury to people or property resulting from any ideas, methods, instructions or products referred to in the content.